ISSN (Print) 1226-1750
ISSN (Online) 2233-6656
Journal of Magnetics 26(1), 71-78 (2021) https://doi.org/10.4283/JMAG.2021.26.1.071

Piezomagnetic Response to the Low- and High-Cycle Fatigue Behavior of X80 Pipeline Steel

Sheng Bao*, Pengfei Jin, Zhengye Zhao, and Yibin Gu

College of Civil Engineering and Architecture, Zhejiang University, Hangzhou, Zhejiang 310058, China

(Received 8 December 2019, Received in final form 26 February 2021, Accepted 8 March 2021)

The goal of this research is to investigate the difference of the piezomagnetic response of X80 pipeline steel caused by low- and high-cycle fatigue. A series of fatigue tests were performed and the piezomagnetic signals were measured. The results show that although the shapes of the magnetic curves for low cycle fatigue and high cycle fatigue are different, the evolution of the curves can be both divided into three stages. The relationship between the experimental results and the theoretical models are discussed. The piezomagnetic response of X80 pipeline steel provides a potential possibility for evaluating the residual fatigue life of the submarine pipeline.

Keywords : pipeline steel, piezomagnetic response, high cycle fatigue, low cycle fatigue

1. Introduction

Fatigue is one of the main causes of the failure of the submarine pipeline. The traditional approach for determining the residual fatigue life is to establish the S-N curves for the materials. However, this method does not track the progressive degradation process of the material [1]. The magnetic properties of the ferromagnetic materials are sensitive to the mechanical and microstructural conditions of the materials. The microstructural changes caused by fatigue may affect the piezomagnetic signals. Therefore, it may be a more effective way to evaluate the residual fatigue life of the submarine pipeline.

Many scholars studied the progressive degradation of ferromagnetic materials under cyclic loading by the evolution of the piezomagnetic field [2-15]. They found the magnetic hysteresis behaviors demonstrated a higher sensitivity to the evolution of fatigue than the corresponding stress-strain hysteresis. The magnetic parameters change along with the fatigue cycles with monotonic linear regularity and show three stages in the fatigue process. These parameters can be used for fatigue damage evaluation of medium carbon steel and prediction of the variation trends of the magnetization of steel bar subjected to cyclic loading. The experimental results demonstrate that the magnetic flux density of the specimens showed three stages in the fatigue process.

Lazreg and Hubert [7] further investigated the relationship between the area of the piezomagnetic cycles and the fatigue life, and they confirmed the piezomagnetic measurement is an effective method of predicting the residual fatigue life of the materials. However, few studies were carried out to investigate the differences of the magnetic signals induced by high cycle fatigue and low cycle fatigue. This research continues the author's prior studies [8], and explores the influences of high and low cycle fatigue failure on the piezomagnetic field. The object of this research is to develop empirical correlations between piezomagnetic responses of X80 pipeline steel with progressive changes that take place during high and low cycle fatigue process.

2. Experimental Detail

The tested material was X80 steel. X80 steel is widely used in deep-water drilling risers. The chemical compositions and mechanical properties of X80 steel are listed in Tables 1 and 2. The specimens are of the same dimensions as shown in Fig. 1.

Fatigue tests were carried out using the INSTRON 8802 testing machine with a peak capacity of 250 kN. A loading frequency of 1 Hz and a sampling rate of 1000 data points per cycle were used. The loading speed was 100 MPa/s. The magnetic signals (B Field) were mea-

*Corresponding author: Tel: +86-571-88208728
Fax: +86-571-88208733, e-mail: longtubao@zju.edu.cn

Table 1. Chemical compositions of X80 steel (wt%).

Material	C	Si	Mn	P	S	Cr	Ni	Mo
X80	0.043	0.21	1.67	0.01	0.003	0.025	0.023	≤0.5

Table 2. Mechanical properties of X80 steel.

Material	Elastic modulus E (GPa)	Yield strength σ_y (MPa)	Ultimate tensile strength, σ_u (MPa)
X80	205	565	650

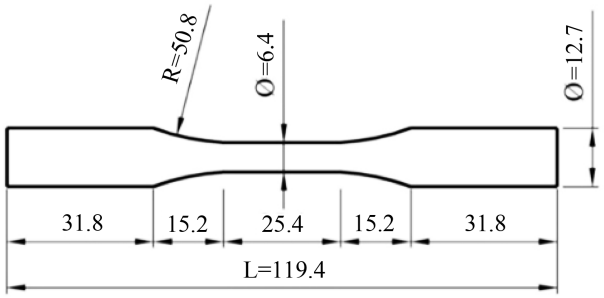

Fig. 1. Fatigue specimen dimensions (unit: mm).

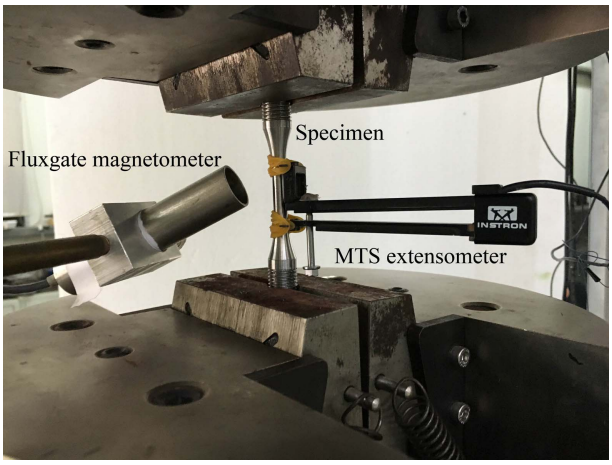

Fig. 2. (Color online) Setup of the magnetic probe.

sured by the fluxgate magnetometer (Model 428D). The sensitivity of the fluxgate magnetometer is 0.1 nT. Rubber bands were used to install the extensometer instead of steel springs to reduce the magnetic field interference. The magnetic field probe shielded by a cylindrical Mu metal tube could only detect the magnetic induction parallel to the cylindrical axis of the probe. The probe was positioned close to the specimen at an angle of 25°, and the distance between the probe and the specimen was 3 mm, as shown in Fig. 2. Tests were run under strain control using symmetric triangular waveforms until the

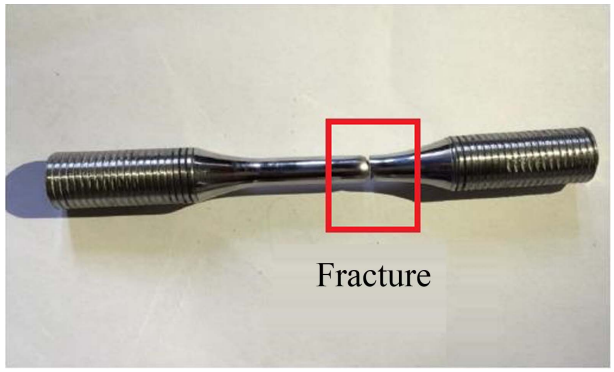

Fig. 3. (Color online) Eventual failure of the specimen.

eventual failure, as shown in Fig. 3.

3. Results and Discussions

The results of two specimens, X80-1 and X80-2, were analyzed. The maximum stress applied to the X80-1 was 460 MPa and the stress ratio was -1. X80-1 was fractured after 4332 cycles, which is a low cycle fatigue failure. The maximum stress applied to the X80-2 was 380 MPa and the stress ratio was -1. X80-2 was fractured after 110020 cycles, which is a high cycle fatigue failure. The differences between the low cycle fatigue failure and the high cycle fatigue failure were discussed.

3.1. Low cycle fatigue failure

Figure 4 shows the evolution of the magnetic-stress

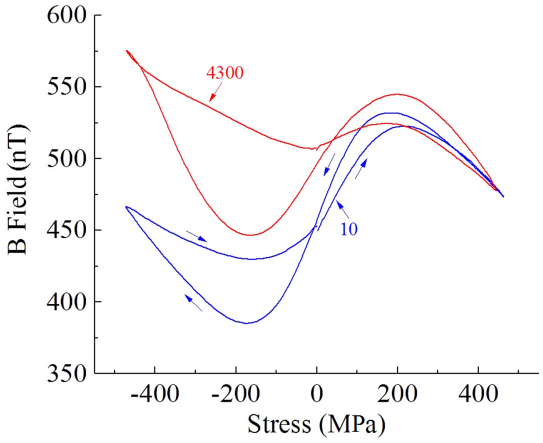

Fig. 4. (Color online) Evolution of the magnetic-stress hysteresis loops of X80-1 for cycle 10 and cycle 4300.

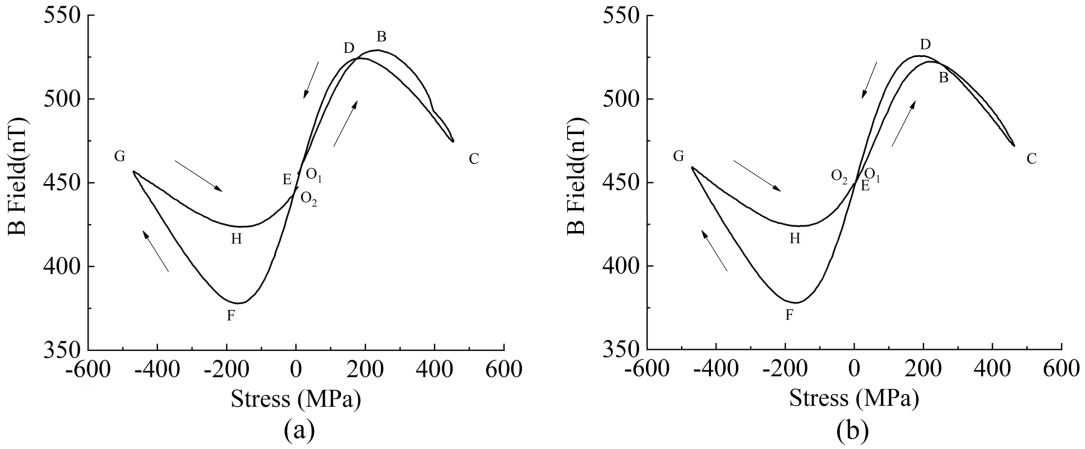

Fig. 5. Magnetic-stress hysteresis loops of X80-1: (a) cycle 1, (b) cycle 2.

hysteresis loops of X80-1 for cycle 10 and cycle 4300. One may observe that when the stress is -460 MPa, the magnetic amplitude has grown by nearly 23 percent and increases from 466 nT in cycle 10 to 575 nT in cycle 4300. As the number of cycles increases, the shape of the hysteresis loop tends to be plumper, which indicates that the piezomagnetic response can reflect the progressive degradation process of fatigue sensitively.

Figure 5 shows the magnetic-stress hysteresis loops of X80-1 for cycle 1 and cycle 2. In Fig. 5(a), one may observe that in the tensile loading branch O_1BC, the B field firstly increases as the tensile stress increases and reaches its maximum point B of 529 nT at the stress of 240 MPa. After that, the B field starts to decrease and reaches its minimum point C of 474 nT at the stress of 460 MPa. In the unloading branch CDE, the B field increases as the tensile stress decreases and reaches its maximum point D of 524 nT, then decreases until the tensile stress decreases to 0 MPa. In the compressive loading branch EFG, the compressive stress was applied to the specimen. It can be seen that the B field decreases as the compressive stress increases and reaches its minimum point F of 378 nT at the stress of -170 MPa. Then the B field increases and reaches its maximum point G. In the unloading branch GHO_2, the B field decreases as the compressive stress decreases, and reaches its minimum point H of 423 nT at the stress of -160 MPa. At last, the B field increases until the compressive stress decreases to 0 MPa. The evaluation of magnetic-stress hysteresis loop shows the magnetization caused by tensile and compressive stress is asymmetric. One may observe that in the tensile stage, the curve of loading branch O_1BC lies above the curve of unloading branch CDE, and the B fields at point B and D differ by only 5 nT. However, in the compressive stage, the curve of loading branch EFG lies below the curve of unloading branch GHO_2, and the B fields at point F and H differ by 46 nT. Additionally, the B fields at point O_1 and O_2 differ by 10 nT, which means the piezomagnetic field does not return to its original value after the stress return to zero again. It can be concluded that the magnetization caused by tensile and compressive stress is asymmetric, which was firstly proposed by Sablik and Schneider [9, 10]. They gave an explanation for this phenomenon that the magnetic domains tend to rotate towards the easy magnetization direction under the tensile stress, however, a part of magnetic domains deviated from the easy magnetization direction under the compressive stress. Therefore, a stress demagnetization factor, $-D_\sigma M$, which is the ratio of the piezomagnetic field of specimen under cyclic compressive stress and tensile stress, can be added in classical J-A model to describe the asymmetry in magnetic behavior under tensile and compressive stress.

By comparing Fig. 5(a) and 5(b), one may observe that the magnetic-stress hysteresis loop for cycle 2 is different from the loop for cycle 1, especially in the tensile stage. In cycle 2, the B field at point B (i.e. 522 nT) is smaller than the B field at point D (i.e. 526 nT), which is opposite to cycle 1. And the difference of the B fields at points O_1 and O_2 is reduced to 3 nT. This can be explained by the law of approach. The applied stress, no matter compressive or tensile, will cause the magnetization to approach the anhysteretic curve.

Figure 6 shows the magnetic-stress hysteresis loops of X80-1 for cycle 50, cycle 150 and cycle 275. In cycle 50, the B field at the minimum stress is 519 nT and the B field at the maximum stress is 469 nT. As the number of cycles increases, the B field at the minimum stress gradually increases, while the B field at the maximum stress gradually decreases. It can be seen that the mag-

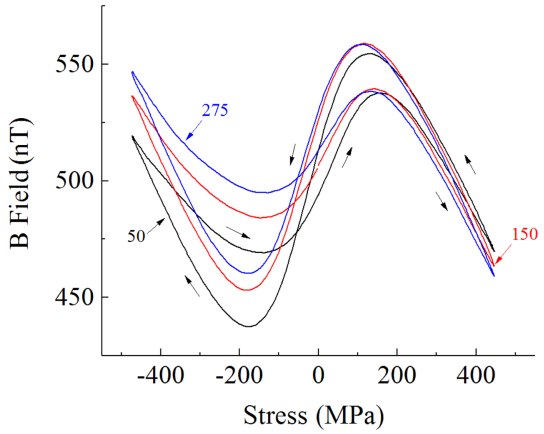

Fig. 6. (Color online) Magnetic-stress hysteresis loops of X80-1 for cycles 50, 150 and 175.

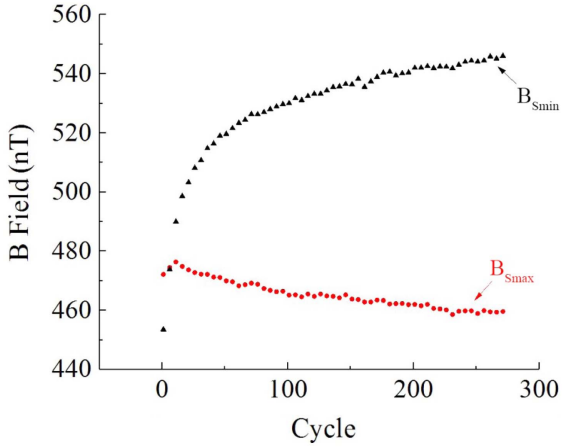

Fig. 7. (Color online) Evolution of B_{Smin} and B_{Smax} for the first 275 cycles.

netic-stress hysteresis loop rotates clockwise around the center of the curve. The B field at the minimum stress—the maximum stress in compression—is denoted as B_{Smin}, and the B field at the maximum stress is denoted as B_{Smax}. The evolution of B_{Smin} and B_{Smax} for the first 275 cycles can be seen in Fig. 7. In the first 66 cycles, B_{Smin} increases quickly at first, and then the increase of B_{Smin} gradually slows down. For cycles 66-275, B_{Smin} increases almost linearly as the number of cycles increases. The variation of B_{Smax} is relatively small. In the first 11 cycles, B_{Smax} increases as the number of cycles increases. However, B_{Smax} decreases as the number of cycles continues to increase. Compared to the increase rate of B_{Smin}, B_{Smax} decreases slowly, which is consistent with Fig. 6.

Figure 8 shows the magnetic-stress hysteresis loops of X80-1 for cycles 2000-2100 and cycles 3500-3600. In the middle stage of the whole fatigue process, the piezomagnetic traces tend to be plumper as the number of cycles

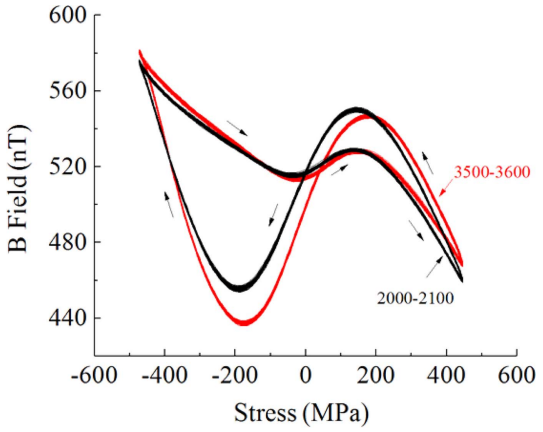

Fig. 8. (Color online) Magnetic-stress hysteresis loops of X80-1 for cycles 2000-2100 and cycles 3500-3600.

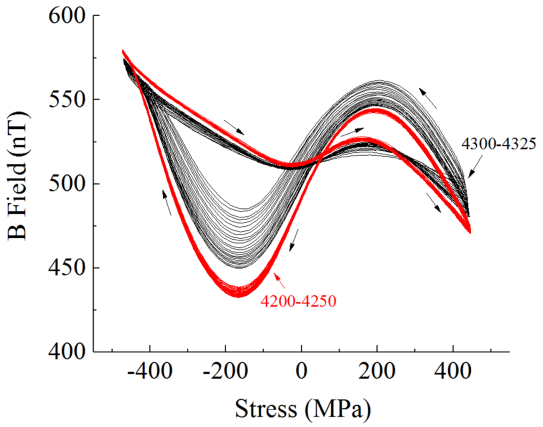

Fig. 9. (Color online) Magnetic-stress hysteresis loops of X80-1 for cycles 4200-4250 and cycles 4300-4325.

increases, especially in the compressive stage. Additionally, the local maximum points in the tensile stage and the local minimum points in the compressive stage for cycles 3500-3600 are lower than that for cycles 2000-2100.

Figure 9 shows the magnetic-stress hysteresis loops of X80-1 for cycles 4200-4250 and cycles 4300-4325. In the final stage of the whole fatigue process, the amplitude of the magnetic field changes sharply. It can be seen that the piezomagnetic traces for cycles 4200-4250 are almost overlapping with each other, while the traces for cycles 4300-4325 are separating from each other. The last three cycles before the eventual failure can be seen in the Fig. 10. The magnetic-stress hysteresis loop cannot maintain its original shape and has a great distortion. For cycle 4330, a local minimum point appears in the tensile stage and the local minimum point disappears in the compressive stage. The curve cannot form a loop at the stress of 0 MPa. The evolution of the curve for cycle 4331 is similar to the curve for cycle 4330. The curve moves down and

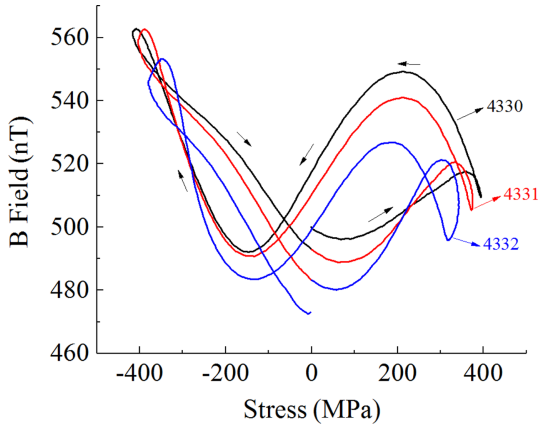

Fig. 10. (Color online) Last three cycles before the eventual failure.

tends to shrink as the number of cycles increases. Cycle 4332 is the last cycle before the eventual failure. It can be seen that the cyclic stresses are reduced to -380 MPa to 380 MPa, which means the specimen reaches its ultimate state.

The magnetic-stress curve changes as the fatigue damage accumulates. Therefore, it is possible to show the accumulation of fatigue damage and the degradation process of materials using the magnetic field. In the fatigue testing, the variations of B_{Smax}, B_{Smin} and their difference, Δ_B, are most obvious, which can be used to evaluate the damage degree of the specimen. Figure 11 shows the evolutions of B_{Smax}, B_{Smin} and Δ_B in the whole fatigue process. The fatigue life can be divided into three stages: initial accommodation, accretion of damage and terminal failure. In order to obtain the transitional points of the stages, the tangent lines of the two adjacent sections of the curve are drawn. The intersection point of the tangent lines is denoted as the transitional point. In the initial stage, B_{smax} decreases rapidly, and then the decrease of B_{smax} gradually slows down as the number of cycles increases. In the middle stage, B_{smax} increases at a low rate. In the final stage, B_{smax} increases rapidly until the eventual failure. On the contrary, B_{Smin} and Δ_B increase in the initial stage, and decrease in the final stage. The point between the initial stage and the middle stage is denoted as N_2, and the point between the middle stage and the final stage is denoted as N_3, as shown in Fig. 11. The total fatigue life of the specimen is denoted as N_f. It can be seen that the N_2 of X80-1 is 521, and the N_3 of X80-1 is 4011. The ratio of N_2 and N_f is 12 %, and the ratio of N_3 and N_f is 92.5 %.

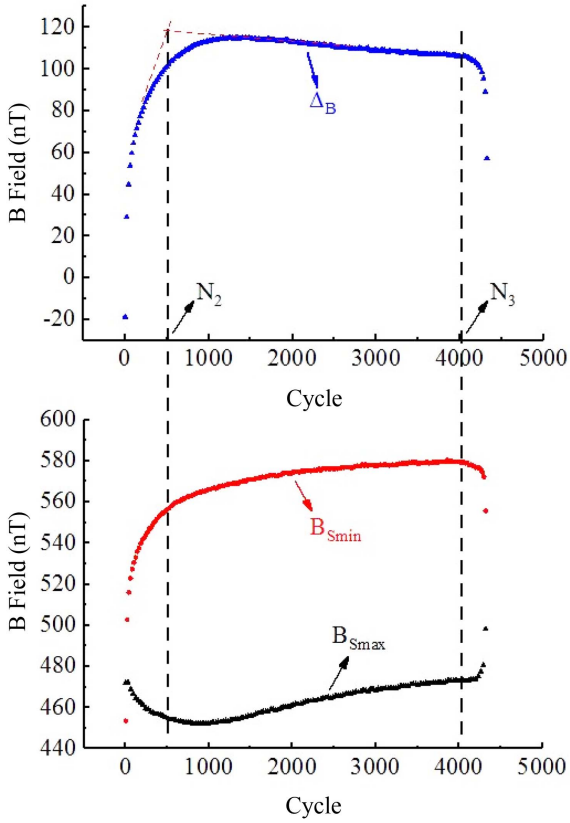

Fig. 11. (Color online) Evolution of B_{smax}, B_{Smin} and Δ_B in the whole low cycle fatigue process.

3.2. High cycle fatigue failure

Specimen X80-2 failed after 110020 cycles, which is a high cycle fatigue failure. Figure 12 shows the magnetic-stress hysteresis loops of X80-2 for the first 100 cycles and the last 100 cycles. One may observe that the loops of the first 100 cycles are much fuller than the loops of the last 100 cycles. Additionally, in the first 100 cycles, there are only two points of intersection at the maximum and minimum stresses. However, the number of intersection points reaches to 7 in the last 100 cycles. It

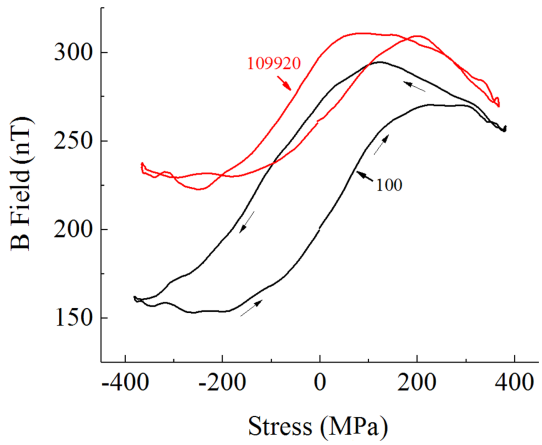

Fig. 12. (Color online) Magnetic-stress hysteresis loops of X80-2 for the first 100 cycles and the last 100 cycles.

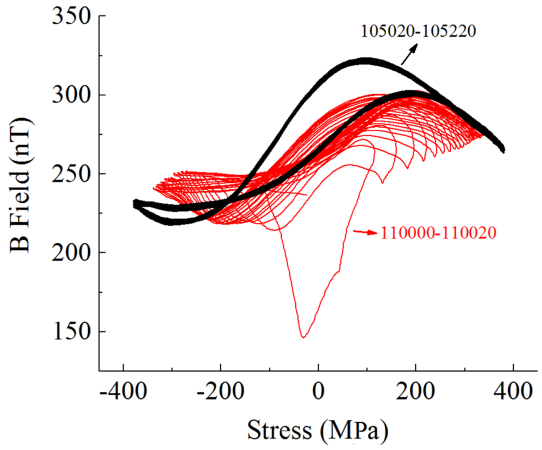

Fig. 13. (Color online) Magnetic-stress hysteresis loops of X80-2 for the last 200 cycles and last 20 cycles.

indicates that as the fatigue damage accumulates, the magnetic-stress hysteresis loop tends to shrink and overlap. By comparing Fig. 4 and Fig. 12, it can be seen that the shape of the magnetic-stress hysteresis loop of X80-2 is quite different from that of the loop of X80-1. The curve of X80-1 intersects at the zero stress, while the distance of the curve of X80-2 is the largest at the same position.

Figure 13 shows the magnetic-stress hysteresis loops of X80-2 for the last 200 cycles and last 20 cycles in the fatigue testing. In the last 200 cycles, B_{Smin} increases from 228 nT to 233 nT, B_{Smax} decreases from 267 nT to 263 nT. The variations of B_{Smin} and B_{Smax} are relatively small. However, in the last 20 cycles, B_{Smin} increases rapidly and B_{Smax} decreases rapidly. The abnormal variations of magnetic signals can be used to predict the final failure of the specimen.

Figure 14 shows the evolutions of B_{smax}, B_{Smin} and Δ_B in the whole high cycle fatigue process. In the initial

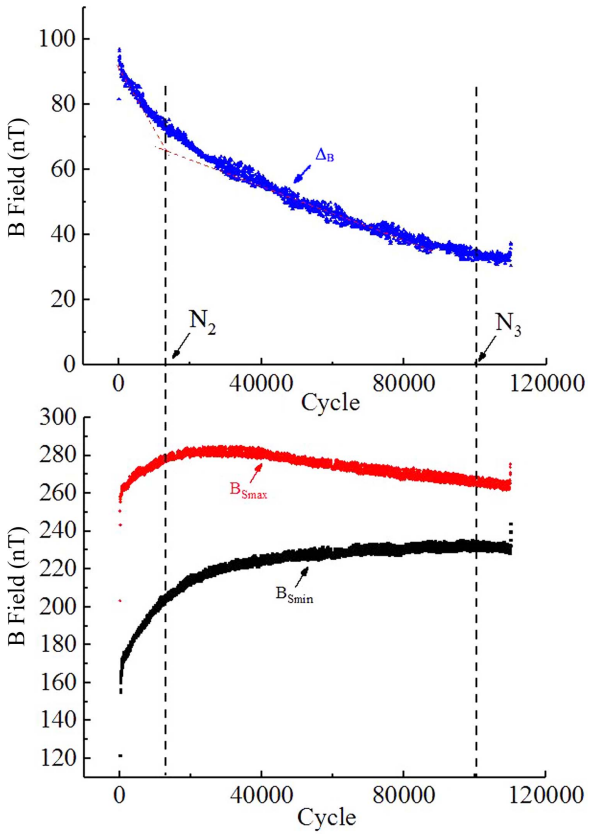

Fig. 14. (Color online) Evolutions of B_{smax}, B_{Smin} and Δ_B in the whole high cycle fatigue process.

stage, B_{smax} and B_{Smin} increase rapidly, but the rate of increase gradually slows down. In the middle stage, B_{Smin} continues to increase as the number of cycles increases, while B_{smax} begins to decrease. In the final stage, both of B_{smax} and B_{Smin} decrease slowly. Δ_B decreases in the whole fatigue process. Different from the low cycle fatigue failure, the high cycle fatigue failure is a brittle

Table 3. N_2, N_3 and N_f of all the X80 specimens.

Specimen No	Minimum stress (MPa)	Maximum stress (MPa)	N_f	N_2	N_3	N_2/N_f	N_3/N_f
X80-1	-460	460	4332	521	4011	12.03 %	92.59 %
X80-2	-380	380	110020	12401	100551	11.27 %	91.39 %
X80-3	-500	500	1168	115	1086	9.85 %	92.98 %
X80-4	-500	500	982	98	912	9.98 %	92.87 %
X80-5	-580	580	254	30	232	11.81 %	91.34 %
X80-6	-460	460	3923	386	3564	9.84 %	90.85 %
X80-7	-420	420	12353	1281	11284	10.37 %	91.35 %
X80-8	-420	420	21538	2059	20054	9.56 %	93.11 %
X80-9	-540	540	909	103	851	11.33 %	93.62 %
X80-10	60	600	338333	31283	\	9.25 %	\
Average						10.53	92.23 %

fracture failure. The magnetic parameters do not show obvious changes in the final stage. The divisions of the three stages are shown in Fig. 14. It can be seen that the N_2 of X80-2 is 12401, and the N_3 of X80-2 is 100551. The ratio of N_2 and N_f is 11.7 %, and the ratio of N_3 and N_f is 91.3 %, which are similar to the ratios of the low cycle fatigue failure.

Table 3 shows the N_2, N_3 and N_f of all the X80 specimens. It can be seen that nearly all the specimens, except the specimen X80-10, show similar three-stage evolutions under different loads. It is noticeable that N_2 and N_3 are easily influenced by the stress, e.g. when the maximum stress is 580 MPa, N_2 of X80-5 is 30 and N_3 of X80-5 is 232. However, when the maximum stress is 420 MPa, N_2 of X80-8 increases to 2059 and N_3 of X80-8 increases to 20054. Interestingly, the ratios of N_2 and N_f of the two specimens are both in the range of 9 % to 12 %, the ratios of N_3 and N_f are in the range of 91 % to 93 %.

Although the shapes of magnetic curves for high and low cycle fatigue are different, there are no obvious differences in the ratios of N_2, N_3 and N_f between the low cycle fatigue and high cycle fatigue. The differences of the shapes of magnetic curves may be induced by the differences of the applied stress. And the influence of the stress on the degradation process of materials is relatively small. In conclusion, as the applied stress increases, the number of cycles decreases, while the ratios of three stages of the fatigue life are constant. SEM can be used to investigate the microstructural change of the materials during the high cycle fatigue process and low cycle fatigue process in the subsequent research.

The above experimental results can be explained by the results of Socha [11]. In the initial accommodation stage (about 10 %), dislocations move and agglomerate, then the crack nucleation occurs. Most fatigue life (about 80 %) is consumed for micro crack initiation and growth. In the last stage (about 10 %), dominant cracks form and develop, leading to the terminal failure. The microstructural changes of the materials during the fatigue process are consistent with the variations of the magnetic signals, which further proves that the piezomagnetic response of the ferromagnetic materials can reflect the accumulation of the fatigue damage.

In order to evaluate the fatigue damage quantitatively, a theoretical model based on the domain wall pining constant, k, is preliminarily proposed. k is a measure of the density of pinning sites and of the energy by which each site is pinned [10], and it is easily influenced by the density of dislocation, ρ.ρ varies with the accumulation of fatigue damage. The ρ of the cycle N can be denoted as ρ_N, correspondingly, the k of cycle N can be denoted as

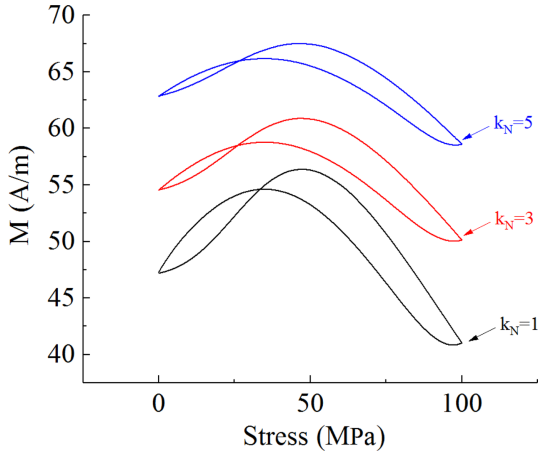

Fig. 15. (Color online) Simulation results when the k_N is 1, 3 and 5.

k_N, and the magnetization strength M of cycle N can be denoted as M_N. The differential equation of M_N and σ can be established as follows:

$$\frac{dM_N}{d\sigma} = \frac{1}{E\xi}\sigma(M_{an} - M) + c\frac{dM_{an}}{d\sigma} - k_N\left(\frac{dM_N}{dH_{eff}}\right) \quad (1)$$

$$M_{an}(H,\ \sigma) = M_s\left[coth\left(\frac{H_{eff}}{a}\right) - \left(\frac{\alpha}{H_{eff}}\right)\right] \quad (2)$$

$$H_{eff} = H + \alpha M + \frac{3\sigma}{\mu_0}[(\gamma_1(0) + \gamma_1'(0)\sigma)M + (2\gamma_2(0) + 2\gamma_2'(0)\sigma)M^3] \quad (3)$$

Where $\gamma_1(0) = 7.0 \times 10^{-8}\ A^{-2}m^2$, $\gamma_2(0) = -3.3 \times 10^{-30}\ A^{-4}m^4$, $\gamma_1'(0) = -1.0 \times 10^{-25}\ A^{-2}m^2Pa^{-1}$, $\gamma_2'(0) = 2.1 \times 10^{-38}\ A^{-4}m^4Pa^{-1}$, $E = 2.1$ GPa, $\xi = 2000$ Pa, $c = 0.1$, $M_S = 1.7 \times 10^6\ Am^{-1}$, $\alpha = 1.0 \times 10^{-3}$, $a = 1.0 \times 10^3\ Am^{-1}$ [12].

Figure 15 shows the simulation results when k_N is 1, 3 and 5. As the fatigue damage accumulates, the dislocation density ρ increases, which causes the increase of k_N. One may observe that the magnetic-stress hysteresis loops move up and shrink as k_N increases, which is consistent with the experimental results in Fig. 12. The relationship between k_N and the number of cycles should be investigated. Further work will focus on establishing a theory model based on k_N to predict the residual fatigue life of the ferromagnetic materials.

4. Conclusions

In this research, high cycle fatigue test and low cycle fatigue test with X80 steels were carried out to explore the piezomagnetic signals induced by cyclic loadings. A comparison of the magnetic variations of high and low

cycle fatigue was made. Three magnetic parameters, B_{Smax}, B_{Smin} and Δ_B, are defined to evaluate the damage degree of the specimen. The evolutions of magnetic parameters for high and low cycle fatigue are different. However, it was found that nearly all the magnetic curves can be divided into three stages: initial accommodation, accretion of damage and terminal failure. The ratios of the three stages to the total fatigue life are about 10 %, 80 % and 10 %. A theoretical model based on k_N to predict the residual fatigue life of the ferromagnetic materials was preliminarily proposed.

Acknowledgements

This work was supported by Public Welfare Technology Research Projects of Zhejiang Province (LGF21E090007), Fundamental Research Funds for the Central Universities (2017QNA4022) and Zhejiang Provincial Natural Science Foundation of China (LZ12E08003).

References

[1] J. T. Han, X. H. Liu, and Z. Y. Jiang, Adv. Mater. Res. **941** (2014).
[2] K. Kida, E. Santos, and M. Uryu, Int. J. Fatigue. **56** (2013).
[3] Y. Chang, J. P. Jiao, X. C. Liu, G. H. Li, C. F. He, and B. Wu, NDT&E Int. 111 (2020).
[4] M. K. Devine, JOM. **44**, 10 (1992).
[5] N. H. Anuar, S. Abdullah, S. S. K. Singh, and A. Arifin, Exp. Tech. (2021).
[6] P. C. Zhang, K. Jin, and X. J. Zheng, JMMM. 514 (2020).
[7] S. Lazreg and O. Hubert, IEEE Trans. Magn. **46**, 2 (2010).
[8] S. Bao and S. F. Gong, J. Appl. Phys. **112**, 11 (2012).
[9] C. S. Schneider, P. Cannell, and K. Watts, IEEE Trans. Magn. **28**, 5 (1992).
[10] M. J. Sablik, J. Appl. Phys. **89**, 10 (2001).
[11] G. Socha, Int. J. Fatigue. **25**, 2 (2003).
[12] J. Zhang and B. Wang, Proc. CSEE **28**, 18 (2008).
[13] L. Vandenbossche and L. Dupre, J. Appl. Phys. **105**, 7 (2009).
[14] T. Erber, S. A. Guralnick, and R. D. Desai, J. Phys. D. Appl. Phys. **30**, 20 (1997).
[15] Y. Melikhov, C. C. H. Lo, and O. Perevertov, J. Phys. D. Appl. Phys. **35** (2002).